Materials Chemistry and Physics 125 (2011) 347–350

Contents lists available at ScienceDirect

Materials Chemistry and Physics

journal homepage: www.elsevier.com/locate/matchemphys

Microwave-assisted synthesis and magnetic studies of cobalt oxide nanoparticles

Aarti Sripathi Bhatt[a], Denthaje Krishna Bhat[a,*], Cheuk-wai Tai[b], Mysore Sridhar Santosh[a]

[a] Department of Chemistry, National Institute of Technology Karnataka, Surathkal, Srinivasnagar 575025, India
[b] Division of Inorganic and Structural Chemistry, Department of Materials and Environmental Chemistry, Arrhenius Laboratory, Stockholm University, S-10691 Stockholm, Sweden

ARTICLE INFO

Article history:
Received 1 April 2010
Received in revised form 25 August 2010
Accepted 3 November 2010

Keywords:
Magnetic materials
Oxides
Nanostructures
Magnetic properties

ABSTRACT

An efficient microwave-assisted route has been used to synthesize nanoparticles of cobalt oxide. The particles were well characterized by transmission electron microscopy (TEM) which showed that the average diameter of the particles is around 6 nm. X-ray diffraction (XRD) studies further confirmed the formation of the spinel Co_3O_4. Purity of the products was detected by Fourier transform infrared spectroscopy (FTIR) combined with thermal gravimetric analysis (TG/DTG). The magnetic measurements revealed a small hysteresis loop at room temperature indicating a weak ferromagnetic nature of the synthesized Co_3O_4 nanoparticles. The magnetic moment of the particles was measured to be 4.27 μ_{eff}.

1. Introduction

Over the past few decades, various synthetic methods have been established for the synthesis of transition metal oxide nanoparticles. In particular, the morphology-controlled synthesis of Cobalt (II, III) oxide (Co_3O_4) with a spinel structure ($Fd3m$) has been extensively investigated. Several technological applications in the field of heterogeneous catalysts [1], solid state sensors [2], electrochromic sensors [3], anode materials in lithium ion rechargeable batteries [4], energy storage [5] and magnetic materials [6] have made Co_3O_4 the main target of material chemists. Because of the influence of the particle size and morphology on the properties of materials, the controlled preparation of the cobalt oxide nanoparticles has become a necessity for the scientists. Thermal decomposition of cobalt precursors [7], chemical spray pyrolysis [8], chemical vapour deposition [9], sol–gel method [10] and solvothermal synthesis [11] are some of the general methods employed to synthesize Co_3O_4. However, these methods are either time consuming or require expensive instruments. Microwave-assisted synthetic route is an appropriate approach under such circumstances; the benefits of narrow size distribution and high purity being the added advantages [12].

The size reduction of metal oxides leads to novel properties which makes them potential materials for applications in various fields. It is anticipated that antiferromagnetic nanoparticles exhibit induced permanent magnetic moments due to lack of internal structural perfection and/or uncompensated spins on the surface of the particles [13]. Co_3O_4 is one such antiferromagnetic material having Neel temperature of ~30 K. They have gained increased attention for exhibiting quantum tunneling of magnetization [14] and in many other applications involving the magnetic quantum effects [15,16]. No wonder in the recent years, research on synthesis and magnetic studies of Co_3O_4 nanoparticles of desired shape and size has gained momentum.

In the present work, we exploit the benefits of the microwave-assisted synthetic route to prepare uniform Co_3O_4 nanoparticles with narrow size distribution. The results show that the experiment yielded high purity Co_3O_4 showing a ferromagnetic behaviour.

2. Experimental

All the chemicals used were of analytical grade and were used as received without further purification. In a typical synthesis, 2 g $Co(NO_3)_2{\cdot}6H_2O$ was dissolved in 10 ml ethylene glycol. To this 8 g of surfactant trioctyl phosphine oxide (TOPO) was added and the solution was sonicated for 30 min to attain homogeneity. The homogeneous solution was then transferred to a Teflon lined vessel and subjected to microwave irradiation (QWave 1000, Questron Technologies Corp., Korea) at high power. The Teflon vessel is connected to an exhaust to drain off any vapours produced during the reaction. After 5 min, a violet coloured solution was obtained, which was centrifuged and washed with acetone and dried at 60 °C. The precursor thus obtained was heated at 40 °C for 3 h in air to finally yield the blackish oxide product.

Investigations on the morphology of the Co_3O_4 nanoparticles and their electron diffractions (ED) were carried out using a transmission electron microscope (TEM, JEOL, 2000FXII) operated at 200 kV. The X-ray powder diffraction analysis was conducted on a JEOL X-ray Diffractometer at a scanning rate of 2°/min with 2θ ranging from 20 to 80°, using Cu K_α radiation (λ = 1.5406 Å). FTIR (THERMO) spectrophotometer has been used to determine the formation of the nanoparticles from the precursor. Thermal analysis was carried out (EXSTAR-6000) from room temperature to 1000 °C at a heating rate of 10°/min under nitrogen atmosphere. The magnetic

* Corresponding author at: Department of Chemistry, National Institute of Technology Karnataka, Surathkal, Srinivasnagar, Mangalore 575025, Karnataka, India. Tel.: +91 824 2474000x3202; fax: +91 824 2474033.
E-mail address: denthajekb@gmail.com (D.K. Bhat).

0254-0584/$ – see front matter © 2010 Elsevier B.V. All rights reserved.
doi:10.1016/j.matchemphys.2010.11.003

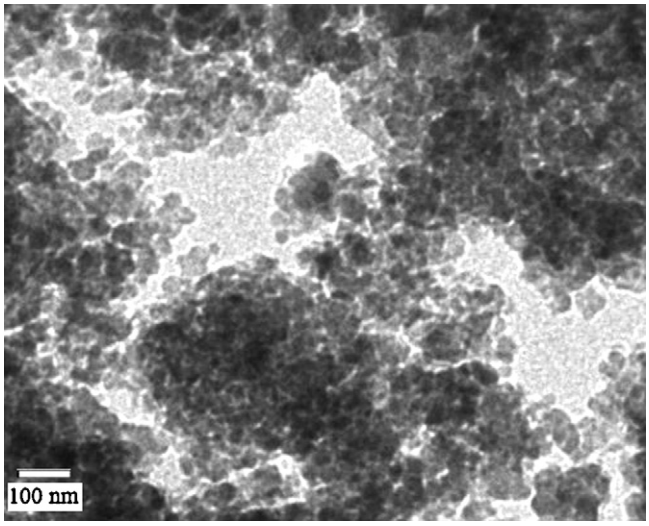

Fig. 1. Bright field TEM image of Co_3O_4 nanoparticles.

properties were assessed with a Vibration Sample Magnetometer (ADE-DMS EV-7 VSM). Magnetic susceptibility of the samples at room temperature was measured by a Magnetic Susceptibility Balance, Sherwood Scientific, Cambridge.

3. Results and discussion

3.1. Transmission electron microscopy (TEM)

The size and shape of the Co_3O_4 nanoparticles were studied by TEM and crystal structure was identified by electron diffraction spectroscopy (EDS). Fig. 1 shows the bright-field TEM images of the sample. The particles show some kind of agglomeration with an average diameter D_{TEM} of 6 nm. Sampling about 150 particles from different TEM micrographs showed that they are almost uniform with a standard deviation of <13%. The particle size data are summarized in Fig. 2. The Polynomial and Gaussian fitment curves in respect of the particle size distribution have also been provided in Fig. 2. As can be seen from the figure, the particle distribution mode is 5 nm and the size of the particles are controlled mostly within 4–8 nm. It is also evident from the figure that more than 67% of the particles are in the range of 5–7 nm and no particle is <2 nm. The orientation of the nanoparticles is random, which is evidenced from the SAED patterns (Fig. 3). The ring patterns indexed in the SAED indicate that the crystal structure is almost identical to bulk Co_3O_4, as further supported by XRD results. Strong reflections of

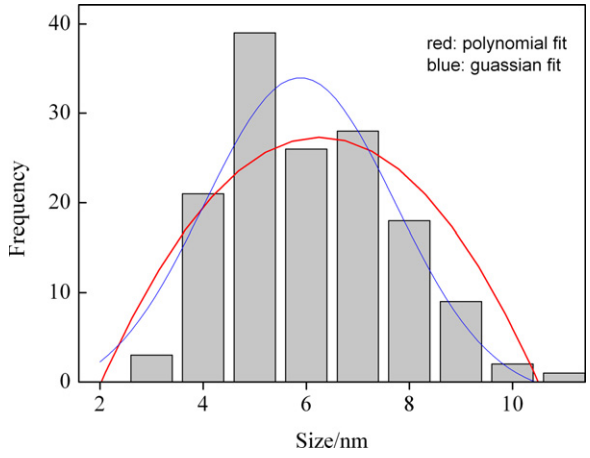

Fig. 2. Size distribution histogram of the sample from TEM analysis.

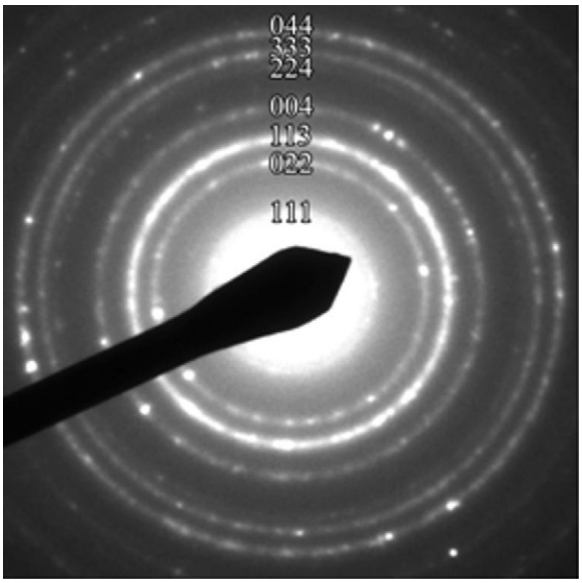

Fig. 3. SAED pattern of Co_3O_4 nanoparticles.

the spinel structure such as (0 2 2) and (1 1 3) are observed. Trace of second phase is found, this may be due to the residual precursors.

The *d* space values measured from SAED patterns are listed in Table 1 along with the values of bulk Co_3O_4 for reference. The values of both samples are similar to the bulk value. The small deviation of lattice parameters from the bulk value is usually found in nanomaterials. The reflection (1 1 1) can be seen but it partially overlaps to the direct beam. The reflections (2 2 2) and (1 3 3) are not observed in the patterns because they are extremely weak in electron diffraction, even in bulk.

3.2. X-ray diffraction studies (XRD)

The XRD pattern of the precursor annealed at 400 °C for 3 h is shown in Fig. 4. The diffraction peaks can be assigned to a cubic phase of Co_3O_4 according to JCPDS 43-1003, indicating the formation of the spinel Co_3O_4. The small peak intensities reveal the nano-size formation of grains.

3.3. Infra-red spectroscopy

The formation of Co_3O_4 phase from the precursor was further ascertained by IR spectroscopy shown in Figs. 5 and 6. In Fig. 5 absorption bands at 2925 and 2856 cm^{-1} corresponding to the C–H stretching vibrations and the peak around 1100 and 1030 cm^{-1} corresponding to the P=O and P–O stretching and bending vibrations are observed. These are particularly due to the presence of phosphine oxide. In the case of Co_3O_4 nanoparticles (Fig. 6) sharp

Table 1
Comparison of *d* space values (Å) for Co_3O_4.

(*h k l*)	This study	Bulk Co_3O_4
(1 1 1)	4.69	4.67
(0 2 2)	2.86	2.86
(1 1 3)	2.44	2.44
(2 2 2)[a]	–	2.33
(0 0 4)	2.02	2.02
(1 3 3)[a]	–	1.85
(2 2 4)	1.66	1.65
(3 3 3) and (1 1 5)	1.56	1.56
(0 4 4)	1.43	1.43

[a] The extremely weak reflection in an electron diffraction pattern.

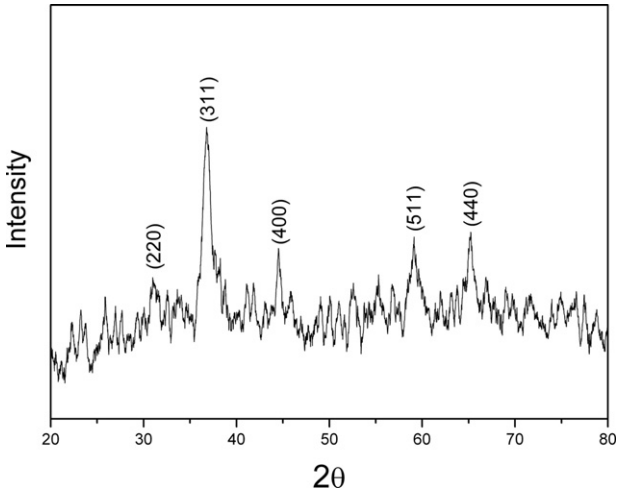

Fig. 4. X-ray diffraction pattern of Co_3O_4 nanoparticles.

absorptions of Co(III)–O and Co(II)–O stretching vibrations at ~570 and 660 cm^{-1} are observed [6]. Very weak absorptions due to P=O and P–O indicate the absorption of phosphate ions on the surface of Co_3O_4 nanoparticles because they could not be washed completely by acetone.

3.4. Thermal analysis

It is known that Co_3O_4 is a thermodynamically stable form under an oxygen containing atmosphere. The stability of the prepared Co_3O_4 was examined under inert gas (nitrogen) atmosphere. The TGA showed a small weight loss (2%) from room temperature to about 160 °C (Fig. 7) which corresponds to loss of structural water and part of the organic decomposition [12]. This is a further evidence of a small amount of surfactant adsorption on the nanoparticles. The TG curve at around 760 °C can be described by the forward reaction of the following equilibrium:

$$Co_3O_4 = 3CoO + 1/2O_2 \quad (1)$$

Conversion of Co_3O_4 to CoO occurs at >760 °C with a DTG peak centered at 845 °C. This is well within the range of 842–858 °C reported by Z.P. Xu and H.C. Zeng for Co_3O_4 to CoO transfor-

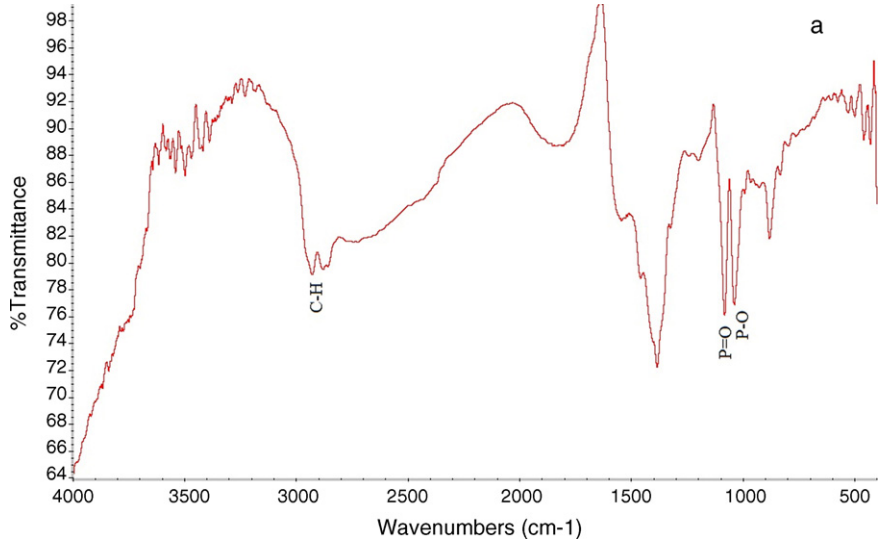

Fig. 5. FTIR spectra of precursor.

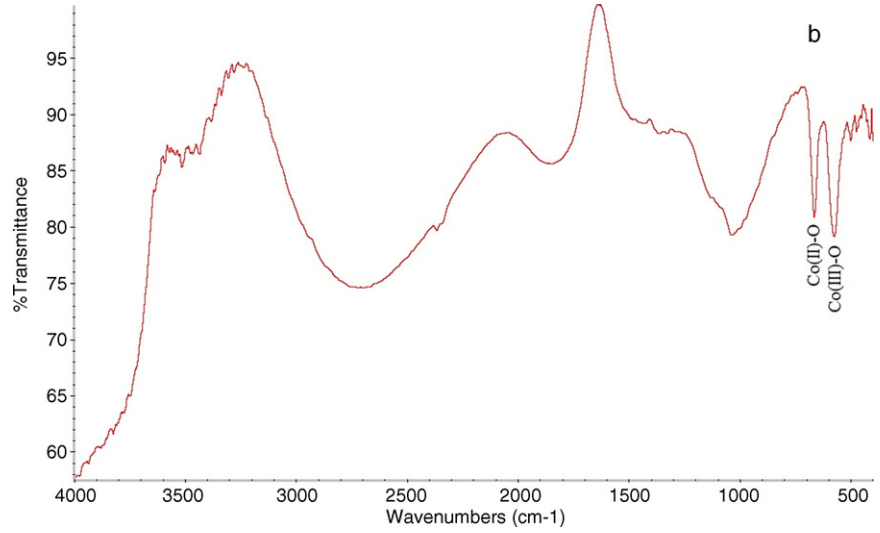

Fig. 6. FTIR spectra of Co_3O_4 nanoparticles.

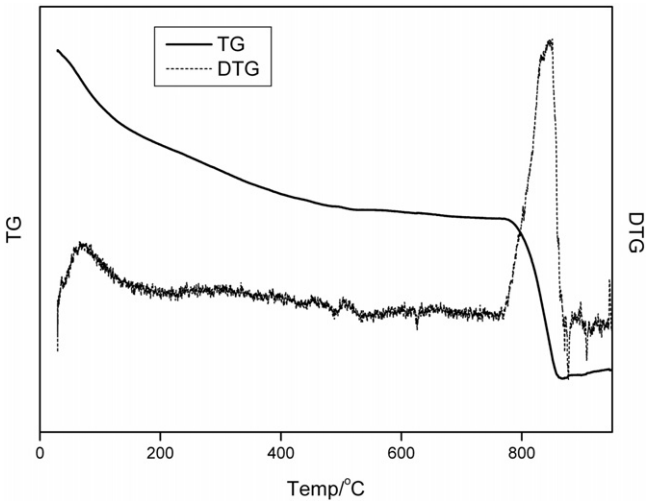

Fig. 7. TG-DTG thermograms of Co_3O_4 nanoparticles in nitrogen atmosphere in the temperature range from 33–1000 °C and heating rate of 10 °C min^{-1}.

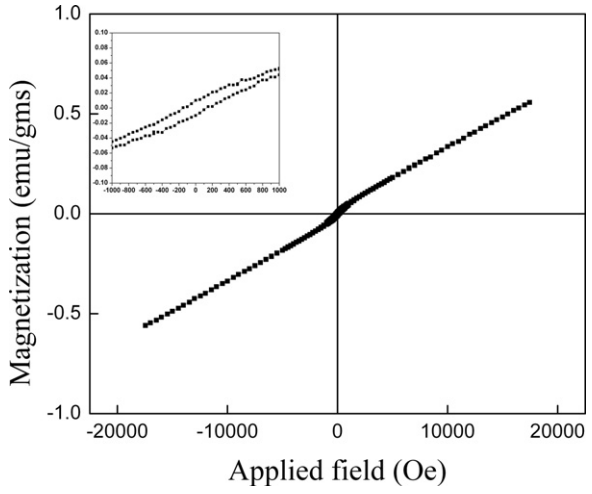

Fig. 8. Magnetization curve as a function of applied magnetic field of nanoparticulate Co_3O_4 at room temperature. The inset shows the magnification of the hysteresis loop.

mation in hydroxide-derived cobalt compounds under nitrogen atmosphere [17].

3.5. Magnetic measurements

Magnetic measurements performed on synthesized Co_3O_4 nanoparticles are presented in Fig. 8. From the figure, a low coercive force and remanent magnetization can be seen, which indicated that Co_3O_4 nanoparticles exhibit a little ferromagnetic property (Fig. 8 inset). The effective magnetic moment per ion μ_{eff} for the nanoparticle was estimated to be 4.27 μ_B. This value is slightly higher than that of bulk crystalline Co_3O_4 (4.14 μ_B) [18]. Makhlouf [19] has reported the effective magnetic moment per ion to be 4.4 μ_B for Co_3O_4 of 20 nm size. The slight increase in the magnetic moment and the ferromagnetic behaviour of the nanoparticles can be explained as follows.

Bulk Co_3O_4 has a normal spinel structure with antiferromagnetic exchange between ions occupying tetrahedral and octahedral sites [18]. It has zero net magnetization due to the complete compensation of sub lattice magnetizations. Hence the change from an antiferromagnetic state for bulk Co_3O_4 to a weakly ferromagnetic state for nanoparticulate Co_3O_4 can be ascribed to the uncompensated surface spins and/or finite size effects [13,20,21]. Also the Co^{3+} ions have no moment at the B sites, while the Co^{2+} ions at the A sites have a permanent moment of 3.25 μ_B as found in neutron diffraction experiments [18]. Due to the small size of the particles, it is possible that a noticeable part of Co^{3+} (d^6 low spin) and Co^{2+} (d^7 ions) switch octahedral and tetrahedral sites, probably by local electron hopping. As a consequence of such a partly inverted spinel structure, the antiferromagnetic interactions between Cobalt ions on the tetrahedral sites do not annihilate [6].

4. Conclusions

In summary, the cobalt oxide nanoparticles have been successfully synthesized by a quick microwave assisted synthetic route using the surfactant TOPO. The synthesized Co_3O_4 nanoparticles were in the size range of 3–12 nm. FTIR and TG measurements showed a negligible amount of the surfactant on the surface of nanoparticles. A small hysteresis loop was observed at room temperature and the value of the effective magnetic moment μ_{eff} was estimated to be 4.27 μ_B. This could be attributed to the uncompensated surface spins and/or finite size effects. The synthetic route can be further used for the synthesis of other transition metal oxides.

Acknowledgements

Financial assistance in the form of an R&D project grant from DST, Govt. of India is gratefully acknowledged. ASB is thankful to NITK Surathkal for the award of a research Fellowship.

References

[1] H. Kim, D.W. Park, H.C. Woo, J.S. Chung, Appl. Catal. B: Environ. 19 (1998) 233.
[2] W.Y. Li, L.N. Xu, J. Chen, Adv. Funct. Mater. 15 (2005) 851.
[3] T. Mruyama, S. Arai, J. Electrochem. Soc. 143 (1996) 1383.
[4] P. Poizot, S. Gurgeon, L. Dupont, J.M. Tarascon, Nature 407 (2000) 496.
[5] S. Noguchi, M. Mizuhashi, Thin Solid Films 77 (1981) 99.
[6] C. Nethravathi, S. Sen, N. Ravishankar, M. Rajamathi, C. Pietzonka, B. Harbrecht, J. Phys. Chem. B 109 (2005) 11468.
[7] W.W. Wang, Y.J. Zhu, Mater. Res. Bull. 40 (2005) 1929.
[8] R.N. Singh, J.F. Koenig, G. Poilleret, P. Chartier, J. Electrochem. Soc. 137 (1990) 1408.
[9] Y. Xuan, R. Liu, Y.Q. Jia, Mater. Chem. Phys. 53 (1998) 256.
[10] M.E. Baydi, G. Poillerat, J.L. Rehspringer, J.L. Gautier, J.F. Koenig, P. Chartier, J. Solid State Chem. 109 (1994) 281.
[11] G. Wang, X. Shen, J. Horvat, B. Wang, H. Liu, D. Wexler, J. Yao, J. Phys. Chem. C 113 (2009) 4357.
[12] Y. Ding, L. Xu, C. Chen, X. Shen, S.L. Suib, J. Phys. Chem. C 112 (2008) 8177.
[13] L. Neel, in: C. Dewitt, B. Dreyfus, P.D. de Gennes (Eds.), Low Temperature Physics, Gordon and Beach, New York, 1962, p. 413.
[14] A. O'Caldera, A.J. Legget, Phys. Rev. Lett. 46 (1981) 211.
[15] S. Takada, M. Fujii, S. Kohiki, T. Babasaki, H. Deguchi, M. Mitome, M. Oku, Nano Lett. 1 (2001) 379.
[16] W. Wang, C.-M. Yang, W. Schmidt, B. Spliethoff, E. Bill, F. Schueth, Adv. Mater. 17 (2005) 53.
[17] Z.P. Zu, H.C. Zeng, J. Mater. Chem. 8 (1998) 2499.
[18] W.L. Roth, J. Phys. Chem. Solids 25 (1964) 1.
[19] S.A. Makhlouf, J. Magn. Magn. Mater. 246 (2002) 184.
[20] T. Ambrose, C.L. Chein, Phys. Rev. Lett. 76 (1996) 1743.
[21] R.H. Kodama, S.A. Makhlouf, A.E. Berkowitz, Phys. Rev. Lett. 79 (1997) 1393.